Chapter 13
Microwire-Based Metacomposites

13.1 Brief Introduction to Metamaterial

13.1.1 Fundamentals of Metamaterials

Metamaterials are one of the most appealing forefront subjects in materials and physics nowadays (see, e.g. [1–6]) in view of the prospect that their successful application may renovate a number of industrial domains such as aeronautics, optoelectronics, and transportation. It has been theoretically and experimentally demonstrated recently that a single microwire or microwire array is capable of metamaterial behaviour; the recent experimental work in our group demonstrates that the polymer composites containing a single array or a crossing array of Fe-based microwires have metamaterial characteristics; we therefore in this chapter focus on this very exciting aspect of microwire composites. Before proceeding, it will be worthwhile to review essential concepts and background information on metamaterials.

A metamaterial is by definition an artificially engineered material that gains its properties from its structure rather than its constituents. The resultant properties, such as negative refractive index and negative stiffness, are not encountered in naturally occurring materials [7]. First of all, a metamaterial must be non-existent in nature, which accounts for the origin of its name, as meta means "beyond" or "of a higher kind" in Greek [8]. It is an extension to the conventional materials in terms of material behaviours. Second, the unique properties of metamaterials are not derived from their constituent materials but from their structure, which distinguishes them from conventional composite materials. Typically, yet not essentially, a metamaterial possesses an ordered structure, realised by a periodic arrangement of the functional units, as schematically depicted in Fig. 13.1. Another implicit rule is that the physical dimensions of unit (scale) and neighbouring distance (periodicity) must be smaller than the incident wavelength so that homogeneity, without which a material cannot be recognised as a "material", can be ensured [7]. The collective responses (effective responses) of all units to the external field (stimuli) give the

H.-X. Peng et al., *Ferromagnetic Microwire Composites*,
Engineering Materials and Processes, DOI 10.1007/978-3-319-29276-2_13

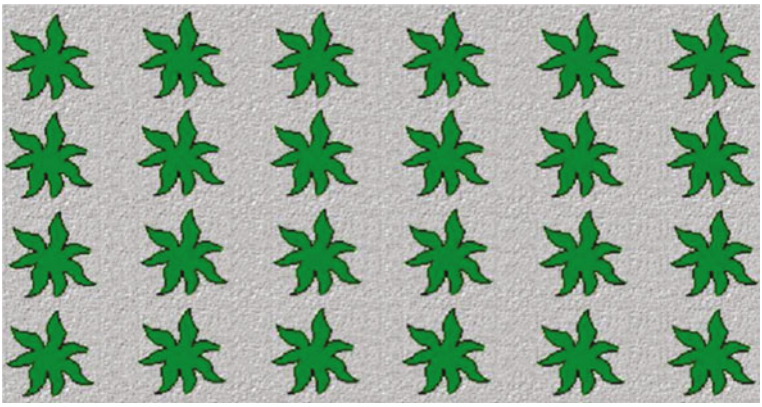

Fig. 13.1 Generic sketch of a volumetric metamaterial synthesised by embedding various inclusions in a host medium

macroscopic properties of a metamaterial. By manipulating the scale and periodicity of these units, one can tailor the properties of a metamaterial. The effective medium theory finds great use herein to study the behaviour of metamaterials, as reviewed in [9], which in turn can be instrumental to metamaterial design and engineering for specific applications. In this sense, metamaterials can also be categorised into smart materials and multifunctional composites.

In this book, the metamaterials are restricted to the electromagnetic metamaterials that are our main interest. An analogy can be drawn between metamaterial engineered by functional units as basic building blocks and the conventional materials composed of atoms. Likewise, Maxwell's equations can be transformed from microscopic to macroscopic form, making it possible to describe the electromagnetic response of a metamaterial via both an effective permittivity ($\varepsilon(\omega)$) and permeability ($\mu(\omega)$). At the subwavelength scale, these two parameters can be manipulated independently and arbitrarily as we desire. Thus, the flow of an electromagnetic wave can be controlled much like a fluid. It follows that some intriguing properties can be achieved for some appropriate materials. For instance, magnetic responses can be realised in metamaterials consisting of mere non-magnetic constituents [10]. At certain frequencies, a negative refractive index material (NIM) can be obtained with both $\varepsilon(\omega)$ and $\mu(\omega)$ being negative ($n = -\sqrt{\mu\varepsilon}$), as depicted in Fig. 13.2. The exploitation of NIMs opens up new prospects of manipulating light and produces revolutionary impacts on present-day optical technologies.

13.1.2 Classification of and Approaches to Metamaterials

Since $\varepsilon(\omega)$ and $\mu(\omega)$ can be controlled independently, it is possible to obtain unusual media with either only negative $\varepsilon(\omega)$ (ENG) or only negative $\mu(\omega)$ (MNG), and both

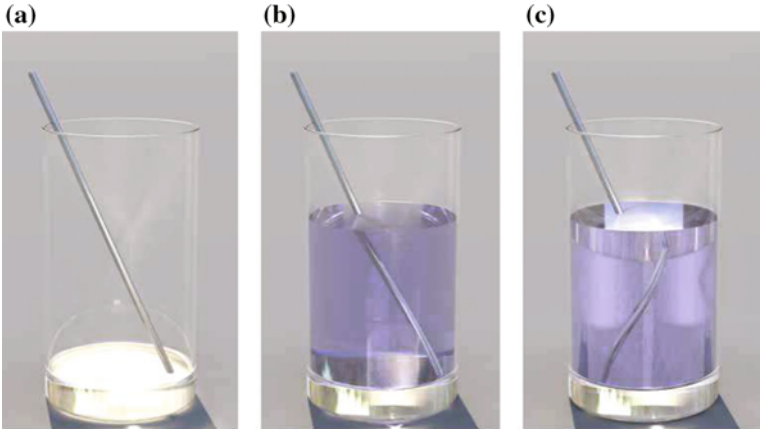

Fig. 13.2 Negative refraction. **a** An empty glass. **b** A glass filled with an ordinary medium with positive refractive index, such as water; the straw inside the glass is refracted. **c** The water is replaced by a negatively refracting medium. Reprinted with the permission from [11], copyright 2006 OSA

of them negative (DNG), as against conventional media with both parameters positive. Such a classification according to the sign of $\varepsilon(\omega)$ and $\mu(\omega)$ is shown in Fig. 13.3, and each class is detailed below.

- **ENG** Many plasmas exhibit this characteristic below plasma frequencies according to the Drude model. Veselago [12] initially proposed gaseous and solid plasmas. Decades later, it was found that noble metallic wires (e.g. silver, gold) behave in this manner in the infrared (IR) and visible frequency domains [2]. This was theoretically proposed first by Rotman and Pendry et al. [13, 14]; Smith et al. [5] and Shelby et al. [4] realised the idea using thin wires as the scattering

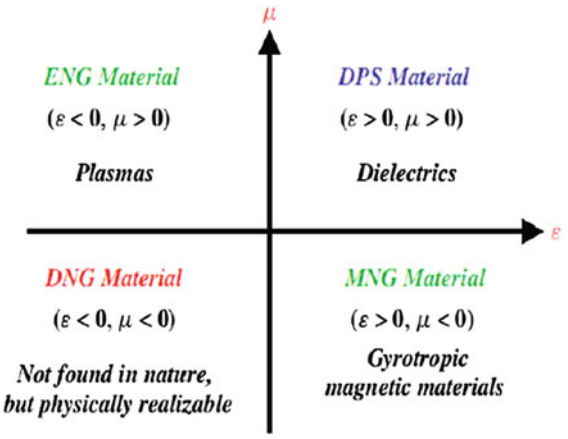

Fig. 13.3 Classification of materials in the $\varepsilon\mu$ plane in terms of their signs. Reprinted with the permission from [3], copyright John Wiley & Sons

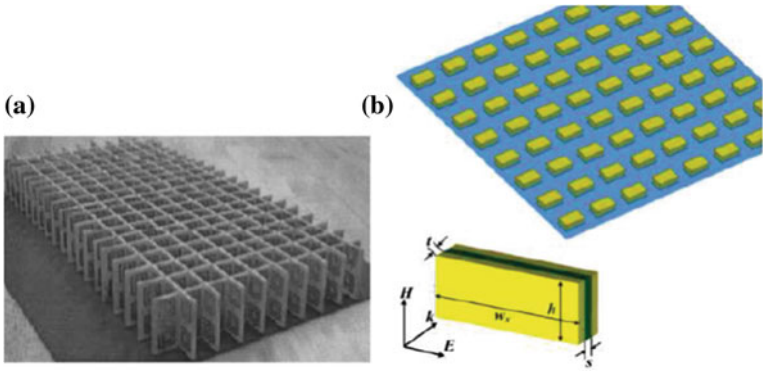

Fig. 13.4 Arrays of SRR structure (**a**) and nanorods (**b**). Reprinted with the permission from [2], copyright 2005 OSA

elements. Composites containing conductive sticks have also been intensively investigated to realise negative permittivity by Lagarkov et al. [15, 16] and Panina et al. [17].

- **MNG** Typical materials of this kind are gyrotropic materials. The composite media with thin wires enabling a resonance feature are also capable of giving negative values of effective permeability near the resonance frequency.
- **DNG** This is also known as a Veselago medium named after its discoverer [12], left-hand material, and NIM. It was realised by Smith and Shelby et al. [5] via split-ring resonators (SRRs), as shown in Fig. 13.4a. It consists of two planar concentric conductive rings, each with a gap. Shalaev et al. [2] also successfully fabricated the NIMs using arrays of gold nanorods or thin wires, as illustrated in Fig. 13.4a.

13.1.3 Applications of Metamaterials

The reason why metamaterials have become a focus of intense study is primarily that they afford a range of novel applications. Perfect lenses proposed by Pendry [1] are one of the most exciting applications. A lossless slab (Fig. 13.5) with a refractive index $n = -1$ projects an image of the object placed into the near field with subwavelength precision. This has profound impacts on biomedical imaging and subwavelength photolithography [18].

Metamaterials are a basis for building a practical cloaking device. The possibility of a working invisibility cloak was demonstrated in [20]. The cloak deflects microwave beams so that they flow around a "hidden" object inside with little distortion, making it appear almost as if nothing were there at all. Such a device typically involves surrounding the object to be cloaked with a shell which affects

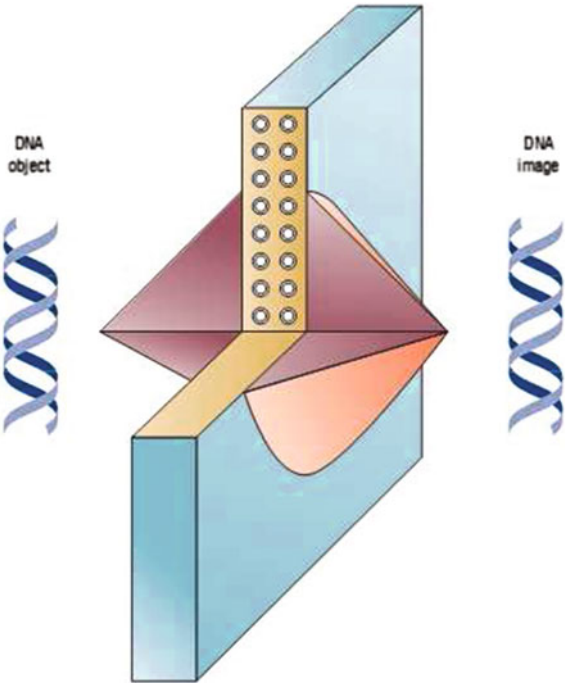

Fig. 13.5 A superlens capable of high-resolution imaging. Reprinted with the permission from [19], copyright 2007 Nature Publishing Group

the passage of light near it. Liu et al. [21] also experimentally demonstrate that a metamaterial cloak is able to revise the reflected waves to make them appear as if reflected from a mirror, thus cloaking the subject behind. Using FE simulations, Cai et al. [22] designed an optical cloaking device which deploys an array of metallic wires projecting from a central spoke that would render an object within the cloak invisible to red light.

Most recently, with an exponential growth of research interest in metamaterials, more potentials are being explored for industrial applications. Sato [23] reviewed the applications of metamaterials in automobiles, as summarised in Fig. 13.6. Melik et al. [24] proposed a metamaterial-based stress sensor with exceptional resolution. Metamaterials are also applied to improve the performance of antennas, as reported, e.g., by Alici and co-workers [25]. The microwave-absorbing capacity of a conventional shielding material can be enhanced by the metamaterial coating, as recently reported by Zou et al. [26]; the metamaterials themselves can also be designed to be perfect absorbers [27], as first demonstrated by Landy et al. [28], who simulated a 99 % absorptivity for a multilayer structure consisting of two metallic layers and a dielectric. Overall, there are still many unknown applications yet to be tapped into for metamaterials. In the present work, arrays of magnetic microwires are employed to obtain negative effective permittivity. Plus, the antiferromagnetic resonance features of ferromagnetic microwires suggest that a

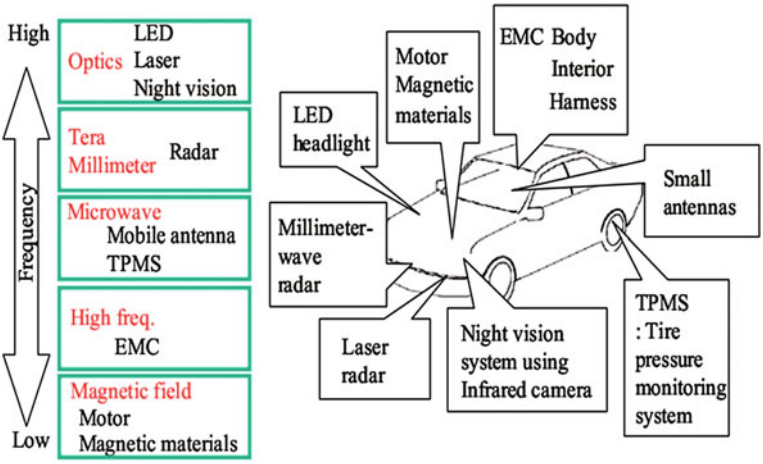

Fig. 13.6 Applications of metamaterials in automobiles [23], reproduced courtesy of the Electromagnetics Academy

negative permeability is also obtainable. In this sense, the microwire composite could demonstrate the metamaterial functionalities, for which corresponding applications are anticipated.

13.2 Metacomposite Characteristics

Thin conducting wire structures are common building blocks for preparing metamaterials with negative permittivity of a range of unusual properties. This has generated a considerable interest in wire media, and a vast amount of literature is devoted to the subject (see, e.g., [29–36]). The negative electrical response also suggests that the wire medium is characterised by a low-frequency stop band from zero frequency to the cut-off frequency, which is often referred to as plasma frequency [37, 38]. For the wire radius on the micron scale, and the lattice constant on millimetre scale, the plasma frequency is in the gigahertz range. In the frequency band above the plasma frequency, the effective permittivity of the wire media enters the negative value region and presents a strong dispersion therein. This may be used to engineer a specific electrical response. However, a single array of non-magnetic wires cannot provide negative magnetic permeability. In order to obtain simultaneously the negative permittivity and permeability, non-magnetic wires are often combined with another array of SRRs [5].

Such design suffers from the drawback of having relatively large dimensions and is not suitable for making into a complex shape when required, e.g., to be made into a coating on a curved surface. Another disadvantage is that such a design is anisotropic and the negative refraction is limited to only a couple of polarisations of

the incident plane electromagnetic wave [39–42], impeding interesting applications such as the perfect lens [1], where an isotropic metamaterial is needed. Most recently, alternative approaches have been proposed capitalising on the magnetic properties of magnetic materials such as ferrites [43, 44], yet during the manufacturing procedure, additional steps are necessary for the combination of non-conducting wires and magnetic materials. This is clearly cumbersome and unappealing for large-scale engineering purposes.

Here comes a question: What is the ideal design for a piece of engineering metamaterial? First of all, the definition of metamaterials is now becoming diverse in that they have covered a range of interdisciplinary subjects and research topics, such as transformation optics [1, 45, 46], electromagnetics [2], and structural mechanics [47]. Yet one key feature remains and is regarded as the centre guideline for conventional metamaterial designs: metamaterials derive their special properties from particular structural effects rather than intrinsic material properties of their constituents [4, 5, 20, 48]. For instance, metamaterials constructed by an array of rods and SRR rings are the most typical prototype. Nevertheless, these existing "metastructures" are not attractive for multifunctional purposes because they lack flexible responses towards external stimuli such as magnetic fields and mechanical stresses. Hence, complicated structures are necessary, albeit unfavourable, to promise the wanted metamaterial properties. Further, it entails a sophisticated fabrication process to guarantee precise dimension control at micro/nanoscales comparable to the concerned wavelength which is a sine qua non for metamaterial design [6, 49]. The downsides confine metastructures for mass production. A remedy is urgently needed.

Enlightened by the beauty of composite materials, we propose a concept of metacomposites where multifunctionalties can be attained from properties of each component. Although the concept has been used by some researchers [50–54], the meaning here is rather different. The metacomposites should meet three essential criteria: (i) a metacomposite is realised by incorporating functional fillers into matrix materials, therefore being a true piece of material with metamaterial features. (ii) Their ultimate properties are dependent on the fillers' material properties apart from structure-associated factors. (iii) They are manufactured via an engineering route.

Ferromagnetic microwires have been recently considered promising for microwave absorption [55, 56] and magnetic sensor applications [57] owing to their distinguished giant magnetoimpedance effect, giant stress impedance effect, and soft magnetic properties [58–60]. Specifically, strong responses from the microwires to the interactive microwave suggest that they can be built into suitable components for applications such as sensing and non-destructive structural health monitoring [61]. In this context, to pursue the most simplified design, a single ferromagnetic wire or array is proposed to provide simultaneous negative permittivity and permeability, in that negative permeability can be obtained at frequencies between the natural ferromagnetic resonance and antiferromagnetic resonance [62–66], while negative permittivity can be obtained below the normalised plasma

frequency $\tilde{f} = f_p/\sqrt{\varepsilon_m}$ [17, 67]. Thus, as long as the ferromagnetic resonance frequency is not higher than the plasma frequency in the continuous-wire case, or the antiantenna resonance in the short-wire case, simultaneous negative permittivity and permeability can be obtained. With a square net configuration, the microwire composite will present isotropic performance. Theoretically, a calculation is given here to illustrate the possibility of obtaining negative permeability and permittivity. For a parallel configuration comprised by conductive wires, the permeability can be expressed as [68]

$$\mu_{\text{eff}} = \frac{1}{2}\frac{(\omega_0+\omega_m)^2-\omega^2}{\omega_0(\omega_0+\omega_m)-\omega^2}\left(1+\sqrt{\left[\frac{\sigma}{\omega\varepsilon}(2\pi\frac{a}{b})^2\right]^2+1}\right) \tag{13.1}$$

where $\omega_0 = \gamma H_{\text{dc}}$ with γ the gyromagnetic constant and H_{dc} the external field. $\omega_m = 2\pi(2\pi\, a/b)2\gamma\, M$ with M the saturation magnetisation of wires of radius a and interwire spacing b and a bulk conductivity σ. For typical values of CoFe–Cr–B–Si wire, $\sigma = 10^{16}$ c^{-1}, $M = 500$ Gs, when $a = 10$ μm, $b = 1$ mm, $H_{\text{dc}} = 10$ Oe, the ferromagnetic resonance is 704 MHz according to $f_r = \mu_0 r\sqrt{H_{\text{dc}}M_{\text{s}}}/2\pi$ [69]. The normalised plasma frequency is 38.9 GHz, when the matrix permeability is 2. In this case, both negative permittivity and permeability are obtained at 1.9–21.7 GHz [68]. It should be noted that by regulating a, b (within the limit) and magnetic bias, the negative index range can be tuned. This could be of great use from the application point of view.

The capability of microwires to realise metamaterial features is demonstrated amazingly in a single wire. Labrador et al. [66] tested a single wire of nominal composition $Fe_{77.5}Si_{12.5}B_{10}$ in a waveguide by paralleling it with the electric field vector on slices of Rohacell foam under a dc magnetic field. Both negative permeability due to the natural FMR and negative permittivity as an effect of interactions with the waveguide are realised in the X-band. Note that, unlike the case of short-circuited microwires with a waveguide, the electrically isolated microwire behaves as if capacitive-loaded, responsible for negative values of the effective permittivity. As the natural FMR occurs at zero magnetic field, a magnetic field is then not an essential element in this metamaterial system, which greatly simplifies its structure. On the other hand, application of a magnetic field could also add the tunable functionality. Such a self-contained and versatile fine element is hence established as a promising metamaterial building block to configure a series of metamaterials, which are discussed below.

Different approaches were developed to realise the metamaterials based on ferromagnetic microwires. Adenot-Engelvin et al. [70, 71] fabricated a wire composite as schematically shown in Fig. 13.7a using CoFeSiB wire with a small negative magnetostriction coefficient of total diameter 9 μm and core diameter 4 μm. The volume fraction of the wires is within the range of 6–11 %. The microwave permeability for this composite is shown in Fig. 13.7b, fitted by a model based on the solenoid approach with a unique set of values for resistance (R), inductance (L), and capacitance (C).

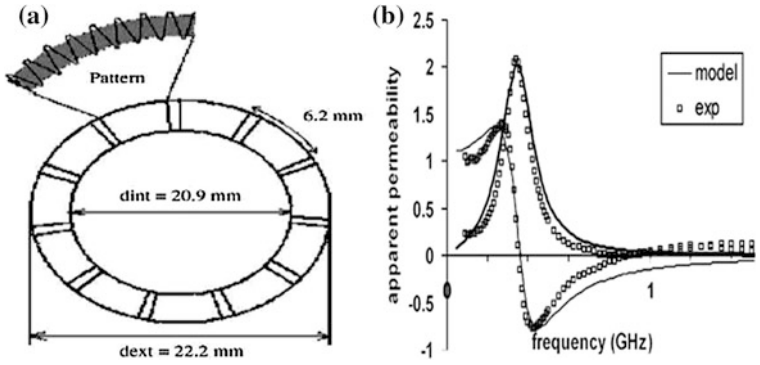

Fig. 13.7 **a** Schematic view of a sample with eleven metamaterial blocks. **b** Measured permeability and model with $R = 0.1$ OΩ, $L = 0.09$ nH, and $C = 9.5$ pF for the eight-loop wire composite. Reprinted with the permission from [70], copyright 2006 Elsevier

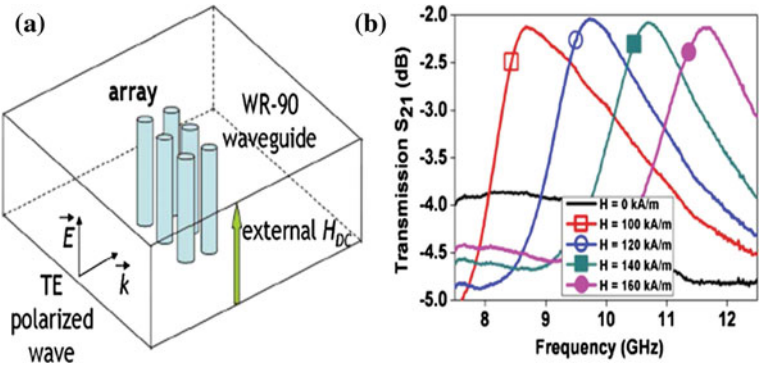

Fig. 13.8 **a** Schematic view of the configuration of wire arrays and measurement set-up. **b** Measured transmission characteristics on an array of two layers of three wires each, as a function of the applied magnetic field H_{dc}. Reprinted with the permission from [62], copyright 2009 AIP

The permeability is also found, in this configuration, to be dependent on the loops, in terms of the resonance frequency by analogy with the magnetic field effect [55, 62] or stress [72]. These field effects can be readily explained by the LLG model for computing the magnetic dynamic susceptibility.

In another configuration (see Fig. 13.8a) [62] constituted by wire arrays of CoSiB with a diameter of 2–3 μm, the transmission spectra were obtained as shown in Fig. 13.8b, exhibiting the rise of transmission with the dc field due to a double-negative condition obtained. Although there is no matrix involved, such wire arrays demonstrate the potential to make metamaterials from these wires. Liu et al. [73] proposed a metamaterial configuration by combining the long conductive fibres along the electric field and microwires along the magnetic field, as shown in Fig. 13.9a. As expected, the negative refraction index is seen at a certain frequency

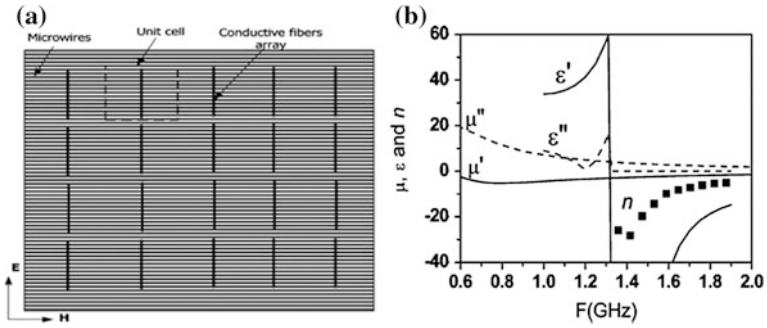

Fig. 13.9 **a** Schematic view of the configuration of composites containing microwires and conductive fibres. **b** Negative refractive index of the microwire composite obtained by HFSS™ [73]

range, as shown in the numerical results (Fig. 13.9b), although the significant resonance loss remains a problem for its application.

A very important sine qua non for realising the metamaterial feature at microwave frequency is that the diameter of the microwire is comparable to the skin depth, as too large a diameter will cause huge reflection [14, 61, 74]. This argument generally holds true for any functions based on microwave/material interactions other than EMI shielding dominated by reflection. For a typical ferromagnetic microwire, $\sigma = 10^{16}$ s^{-1}(10^5 S/m) and $\mu = 20$, the calculated skin depth δ at 10 GHz is about 1 μm [75]. Since the permeability decreases with the frequency, δ changes little. This is larger than even very thin microwires with a typical radius of few microns. Although it is still possible to penetrate into most of the inner core in the Fe-based wire [76] or the outer shell in the Co-based wire [77], the submicron wires [78–83] or nanowires [84–95] would be preferred in this case. On the other hand, reducing the wire diameter will reduce the volume fraction of wires and hence the permittivity and permeability. One may have to accept that such an unavoidable loss is typical for metal metamaterials [96]. Another restriction is set on the "dilute" condition, i.e. $b \gg a$, which is necessary to have a relatively smaller carrier density and large effective carrier mass, such that the plasma frequency can be regulated in the 1–10 GHz range of application interest. The band-stop or band-pass filter, for example, can be designed based on the criticality of plasma frequency on transmission [14, 68]. Also, it is argued that a large number of wires are deleterious since they will absorb most of the electromagnetic wave [64, 72]. This issue must be addressed before the microwire composites can find metamaterial applications such as cloaking. On the other hand, it is desirable for microwave absorption application and field-tunable devices arising from decent dielectric permittivity variation with the presence of external magnetic bias (Fig. 13.10). As such, these two functionalities cannot be pursued simultaneously, but this would greatly extend the freedom of tailoring the electromagnetic properties of the microwire composites.

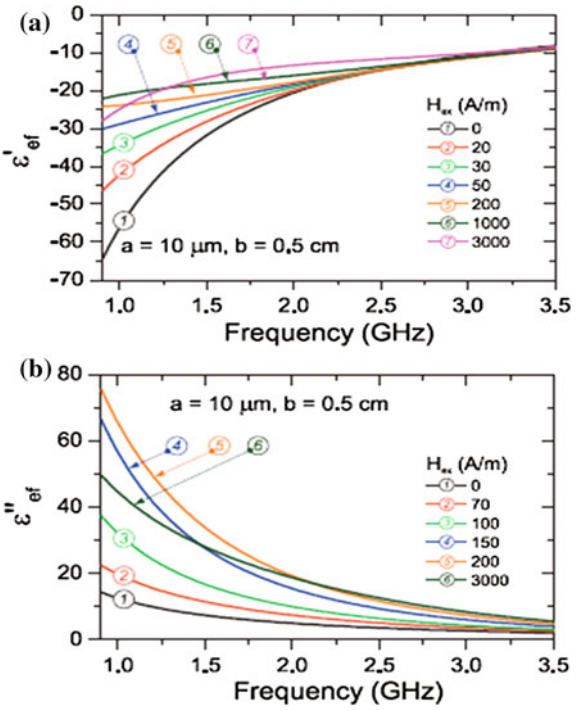

Fig. 13.10 Effective permittivity spectra of $Co_{66}Fe_{3.5}B_{16}Si_{11}Cr_{3.5}$ continuous-wire arrays deduced from the scattering spectra with the external magnetic field as a parameter (wire radius a = 10 μm, spacing between wires b = 5 mm). Reprinted with the permission from [78], copyright 2011 John Wiley & Sons

It should be addressed that above microwire-enabled metamaterial features are still obtained from a pure structure. Although their fascinating properties are derived from their magnetic properties, they are not a composite material in a strict sense. On the other hand, so far all the reports on the ferromagnetic microwire metamaterials are yet limited to the Co-based wires. As is known, Fe-based wires have significantly different domain structure from Co-based wires arising from the positive magnetostriction, and as a consequence, its static and dynamic electromagnetic responses are also distinct from those of Co-based wires [55, 76]. Besides, the natural ferromagnetic resonance (NFMR) of Fe-based wires enables negative permeability dispersion above the FMR frequency, which creates additional degrees of freedom in designing double-negative metamaterial band. In addition, as compared to Co-based wires, Fe-based wires are cost-effective and therefore more desirable for practical applications [58], especially in sensors and transformers. Hence, it is believed that by employing Fe-based microwires alone in a periodical fashion and by incorporating into a high-performance base material, these metamaterial properties can be maintained and new dimensions of functionalities can be realised. Most importantly, this design makes our metacomposites a true piece of material and it is of engineering interest.

Recently, Luo and Qin et al. [97] successfully realised prepreg-based metacomposites containing parallel Fe-based microwire arrays. Experimentally, glass-coated FeSiBC wires were embedded into aerospace graded 950 prepregs

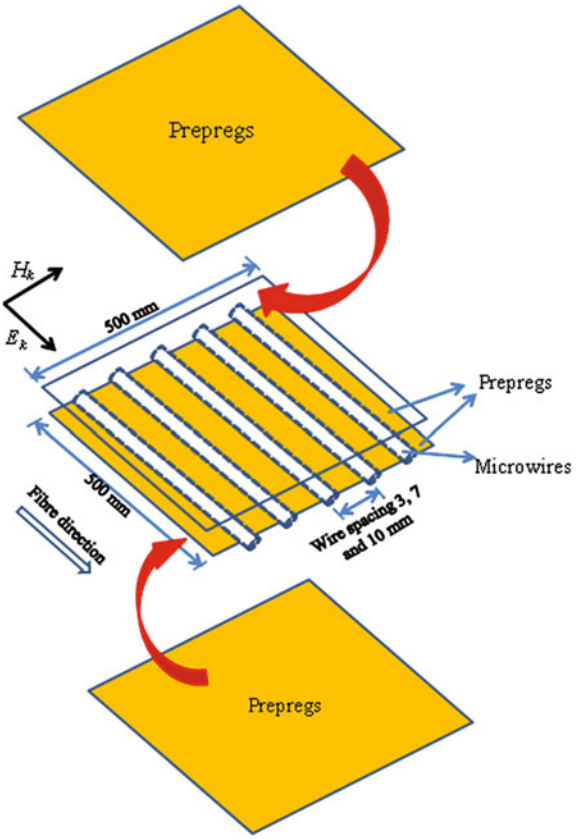

Fig. 13.11 Schematic illustration of the process for manufacturing composites containing Fe-based microwires in parallel manner with wire spacing of *b*. Reprinted with the permission from [99], copyright 2014 AIP

with spacing of 3, 7, and 10 mm, respectively (Fig. 13.11), followed by a hand laying-up and a standard autoclave curing procedure. All the resultant composite samples have an in-plane size of 500 × 500 mm^2 and a thickness of 1 mm. Microwave characterisation was carried in a free-space set-up in 0.9–17 GHz with the presence of a dc magnetic field up to 3 k Oe wherein S-parameters were extracted [61, 98]. Dielectric permittivity was later on calculated from S-parameters via a built-in programme Reflection/Transmission Epsilon Fast Model.

Remarkably, some transmission windows are identified in the 1–7 GHz from the composites containing 3-mm-spaced microwire array (Fig. 13.12a), together with reflection dips and absorption peaks (now shown here). From the permittivity spectra of the same wire composites, one observes that permittivity has negative values below a featured frequency of 16 GHz (Fig. 13.12b), i.e. f_p. From electromagnetic theory, one notes that transmission windows are a typical result of abnormal dispersion and this could be induced by either double-positive or double-negative indices (permittivity and permeability). The observation of negative permittivity denies the former situation, and herein, we can conclude that a negative ε and a negative μ are simultaneously obtained as a metacomposite feature.

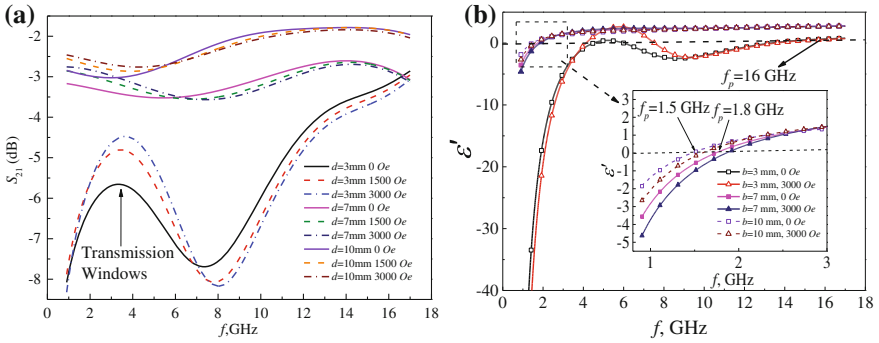

Fig. 13.12 Frequency dependencies of **a** transmission (S_{21}) coefficients and **b** dielectric permittivity of parallel microwire composites with the presence of fields up to 3 k Oe of different wire spacing, b = 3, 7, and 10 mm, respectively. Reprinted with the permission from [97], copyright 2013 AIP

The negative ε is observed below the f_p derived from the parallel alignment of wires [14], while a profile of negative μ is originated from the FMR of wires [58]. Notably, this transmission window can be excited without external magnetic fields, which is also defined as natural DNG feature. This remedies the metastructure consisting of Co-based wire arrays where DNG indices can only be observed in the presence of burden magnets [64]. The designed wire metacomposites renovate the area of realising DNG characteristics where only a simply parallel architecture is needed and can be oriented for microwave cloaking and sensing applications.

Moreover, the transmission windows can only be obtained when the wire–wire spacing is below a spacing of 7 mm. This links to the wire–wire magnetic interaction and the modulation of f_p. From Fig. 13.12b, one observes that when the wire spacing is larger than 3 mm, the plasma frequency is significantly lower than the theoretical prediction. In a wire media, f_p can be described as $f_p^2 = \frac{c^2}{2\pi b^2 \ln\left(\frac{b}{a}\right)}$[14], which is determined by the wire radius a and spacing b. We obtain f_p of 4.8, 6.6, and 16.6 GHz for composites with wire spacing of 10, 7, and 3 mm, respectively. However, from the inset of Fig. 13.12b, we notice that there is a large discrepancy between these calculated values and the experimental ones when the wire spacing is larger than 3 mm, i.e. 1.4 GHz for b = 10 mm and 1.6 GHz for b = 7 mm, respectively. This is arising from the fact that in the above equation, a is the effective diameter that contributes to the overall dielectric response and for microwires, the major response comes from the outer shell of the whole domain structure [14]. Nonetheless, for Fe-based wires, the outer shell volume only occupies a trivial portion [58, 100] such that the final f_p is greatly compromised. Decreasing the wire–wire spacing to a critical value of 3 mm, dynamic wire–wire interactions provide essential offsets to the effective diameter, hence plasma frequency considering the modification of wires' domain structure and magnetic tensor due to the long-range dipolar resonance [76, 101, 102]. It should be stressed

that here the interactions are referred to the dynamic magnetic interactions resulted from the coupling with electrical component of incident waves rather than the magnetostatic coupling, since 3-mm spacing is still too wide to induce meaningful magnetoelastic energy [103, 104].

However, due to the loss generated by the wires, the transmission level is not greatly favourable in this parallel metacomposites. The root cause is the relatively high wire concentration in the case of 3-mm spacing. To overcome the drawback, the same group comes up with an orthogonal array design that is capable of realising the transmission window at much larger wire spacing and providing a much higher transmission level. The orthogonal metacomposites are illustrated in Fig. 13.13. Fabrication and characterisation are detailed elsewhere.

Notably, transmission windows are realised in 1–6 GHz in the metacomposite containing 10-mm-spaced orthogonal microwire array (Fig. 13.14). Furthermore, such configuration attains a higher microwave transmission level yet with a much lower wire content compared with parallel metacomposites filled with wires of 3-mm spacing. This is attractive for miniaturised cloaking devices. Interestingly, one notes that the critical spacing for orthogonal configuration (10 mm) is larger than parallel metacomposites (7 mm); that is, metamaterial features are readily available in orthogonal metacomposites as the spacing is over 10 mm. The 90 degree wires can be regarded as an insertion of an array of discontinuous wires between neighbour continuous 0 degree wires due to small excitation from the axial component of electrical field [105]. The "imaginary" short-cut wires enhance the

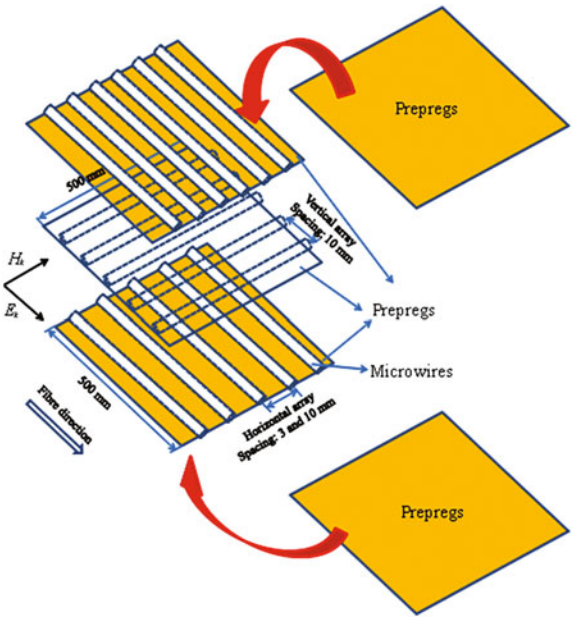

Fig. 13.13 Schematic view of manufacturing process of orthogonal wire array metacomposite with fixed wire spacing 10 mm perpendicular to glass fibres and different horizontal wire spacing of 3 and 10 mm, respectively. Reprinted with the permission from [99], copyright 2014 AIP

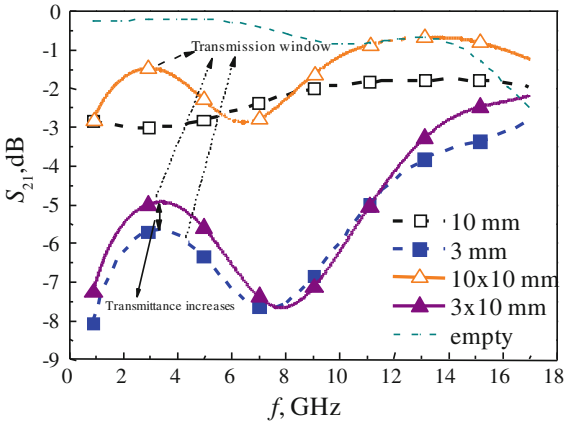

Fig. 13.14 Frequency plots of transmission spectra of polymer composites with parallel and orthogonal wire arrays and blank composite (with no wires) with electrical component along glass fibres in the absence of external fields. Reprinted with the permission from [99], copyright 2014 AIP

wire–wire interaction via the generation of circumferential fields such that the critical spacing is reduced.

Another feature of 3-mm-spaced orthogonal metacomposites is that their transmission is slightly higher than that of the parallel metacomposites with the spacing. This is also attributed to the influence of 90° wire array. In the orthogonal configuration, the small axial component of 90° wires along the electrical field of incident waves enhances both the dielectric permittivity and the magnetic permeability to a similar extent, taking into account the creation of circumferential fields [105]. Furthermore, an extra portion of permeability increase can also be secured via the weak interaction between 90 degree wires and magnetic component in microwaves [55]. Together, the impedance match is improved as per $Z = (\mu/\varepsilon)^{1/2}$, which determines the higher transmission level of orthogonal metacomposites. In this sense, one sees the possibility of a quantitative control of transmission level in the realm of orthogonal metacomposites via the investigation of relation between the transmission increase and amount of 90° wires. This is instrumental to developing cloaking devices out of the microwire composites to reach a required transmittance level from microwave perspective.

So, what is the remaining challenge? If scrutinising the S-parameter spectra of parallel and orthogonal metacomposites, one is able to find that tuning those observed transmission windows is still a tricky issue. Previous studies on meta-metastructures based on Co-based microwires have revealed unique advantages including tunable properties towards fields and stresses [98, 106, 107], thanks to their excellent soft magnetic properties and giant magnetoimpedance (GMI) effect. Absorbing the essence, one naturally comes up with an idea to explore that by incorporating Co-based microwires, how they will interplay with the existing

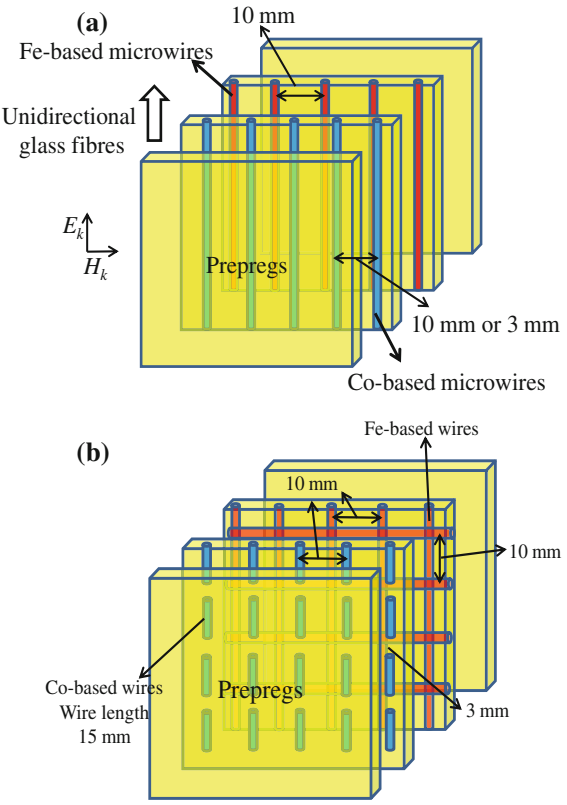

Fig. 13.15 Schematic illustration of the hybridisation of **a** continuous parallel Fe-based microwire array plus continuous Co-based microwire array and **b** orthogonal Fe-based microwire array plus short-cut Co-based microwire array

Fe-based arrays in the composites. Besides, the hybrid metacomposites containing Fe- and Co-based wires would be an interesting topic to investigate how the interactions between Co–Co, Fe–Co, and Fe–Fe wires would influence the transmission windows. Most recently, Luo et al. [108] select two combinations of Fe-based and Co-based microwires, i.e. parallel Co-based and parallel Fe-based wire array (Fig. 13.15a) and short-cut Co-based and continuous orthogonal Fe-based wire array (Fig. 13.15b). We will not harangue the experimental details, yet it should be emphasised that Fe- and Co-based microwires must be embedded into separate prepregs to minimise large reflection losses caused by physical wire contacts otherwise.

From the transmission spectrum of hybrid metacomposite with high wire concentration (10- and 3-mm spacing for Fe- and Co-based wires, respectively) (Fig. 13.16a), one striking feature is that a transmission window emerges with the presence of magnetic field of 300 Oe in the frequency band of 1–3.5 GHz. This suggests that an abnormal transmission dispersion is constructed in the continuous hybridised Fe-/Co-based wire composite system, which is distinct from the previously reported natural transmission windows independent of magnetic field but rather controlled by a critical spacing in the single Fe-based wires containing

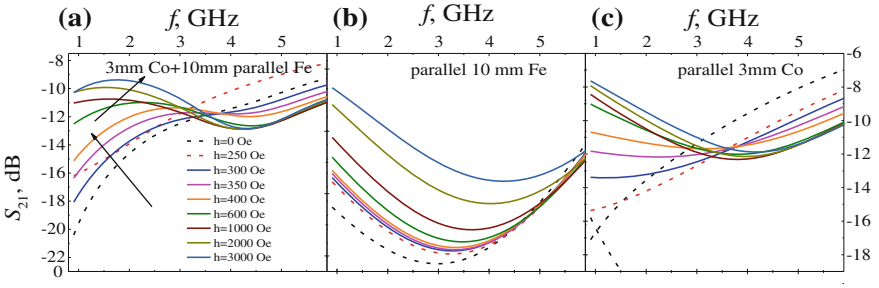

Fig. 13.16 Frequency plots of the transmission coefficients, S_{21}, of composite samples containing **a** hybrid wire arrays with 3-mm-spaced Co-based wires, **b** pure Fe-based wires, and **c** pure Co-based wires

composites [97]. With the evidence of negative permittivity dispersion in the same frequency band and negative phase velocity (not shown here for brevity), it is validated that a magnetic bias-induced double-negative features are obtained. Further, with the external fields increasing, the transmission window peak experiences a redshift–blueshift evolution (Fig. 13.16a). It is implied that such effect is because that the long dipolar resonance dominates at low magnetic fields of 600 Oe, which is induced by the interaction between wire couples [97, 99], and the FMR of Fe-based wires prevails at higher fields than 600 Oe. This magnetic bias-tunable metacomposite behaviour satisfies such working requirements of the microwave invisibility cloaking that can be activated or deactivated by conveniently exerting an additional magnetic field.

However, it should be addressed that at frequencies above 6 GHz, such field-tunable metacomposite behaviour is suppressed due to high reflection loss from the closely packed Co-based wires. Thus, it is natural to realise that, by increasing Co-based wire spacing to 10 mm, a high-frequency transmission window could be attained in the continuous hybrid composite system arising from the possible magnetic resonance between Fe–Co wire couples. A low-frequency transmission window is revealed in the frequency band of 1.5–5.5 GHz without the presence of external fields (Fig. 13.17a), indicating a natural DNG characteristic. This feature resembles the metamaterial feature realised in the parallel metacomposites containing Fe-based wires [97, 99], and readers are reminded of FMR of Fe-based wires and their parallel arrangement in the present case, which are the reasons of the simultaneous achievement of negative permittivity and permeability. Another feature of note is that a transmission enhancement is also achieved at a higher frequency band of 9–17 GHz for such widely spaced wires containing metacomposites, indicating a DNG band (Fig. 13.17b). This is due to the interactive magnetic resonance between Co–Fe wire couples (Co- and Fe-based wires are intentionally mismatched by 1 mm), which is in favour of a negative permeability dispersion in the concerned frequency range. Compared with the metacomposites containing 3-mm-spaced Co-based wires, the hybridisation of a “dilute” microwire array into the composites enables a new way of broadening the metamaterial

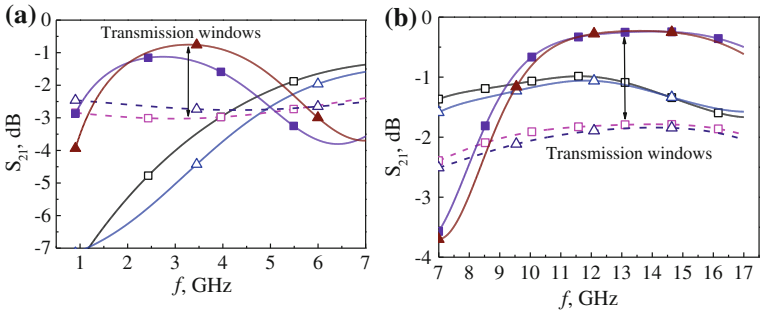

Fig. 13.17 Transmission coefficients of composites containing 10-mm-spaced Fe-based wire array, the 10-mm-spaced Co-based wire array, and their hybridised wire arrays in the frequency band of **a** 0.9–7 GHz and **b** 7–17 GHz

operating frequency band and gives us a paradigm of dual-band metamaterial in the context of composite materials. In a brief conclusion, the spacing of Co-based wires has profound effects on the metamaterial behaviour of wire composites: (i) the magnetic field-tunable properties could only be preserved by significantly decreasing the spacing of Co-based wire array to 3 mm; (ii) increasing Co-based wire spacing can mitigate high reflection loss at high frequencies and induce additional magnetic interaction between Fe–Co wire couples, thus developing a high-frequency transmission enhancement.

Luo and Qin et al. also propose and fabricate an architecture of the combination of orthogonal and short-cut wire arrays [108]. The S-parameters of metacomposites containing, respectively, short-cut Co-based wires, orthogonal Fe-based wires, and their hybridised wire array are shown in Fig. 13.18. Observation of a typical band-stop feature accompanied by a sharp transmission dip and an absorption peak at 6 GHz is identified in the composite containing short-cut Co-based wires. It can be explained by the dipolar behaviour of the short wires. It is established that short wires act as dielectric dipoles when interacting with the electrical component of waves. The dipole resonance can be written as $f_{\mathrm{dr}} = \frac{c}{2l\sqrt{\varepsilon_m}}$ (below the percolation threshold), where ε_m and l denote the permittivity of matrix materials and wire length, respectively [109]. Taking ε_m as 3 [110, 111] and l as 15 mm into above equation, we obtain f_{dr} = 5.8 GHz, which coincides well with the identified resonance peak in Fig. 13.18b. In other sense, the artificial microwave opaqueness in the short Co-based wire composite is induced by the wire configuration therein since no wires' material properties need to be considered. By including such short-cut array into the Fe-based wire–enabled metacomposites, one notes that the observed band-stop feature is maintained along with some enhancement of transmission in the 1–6 GHz frequency (Fig. 13.18a) regime compared with composites containing only orthogonal Fe-based wires. Hence, the introduced short-cut Co-based wires can apply a synergistic influence to enhancing the DNG feature of metacomposites; this is due to the low absorption loss of Co-based wires at DNG

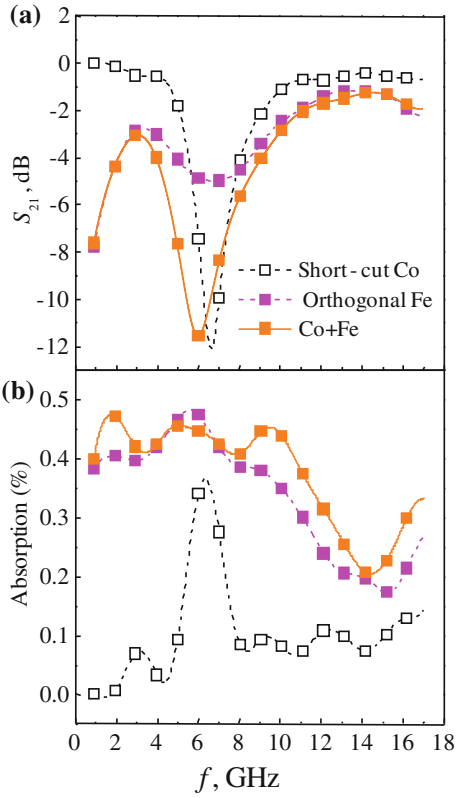

Fig. 13.18 **a** Transmission, S_{21}, and **b** absorption coefficients of composites containing orthogonal Fe-based wire array, short-cut Co-based wire array, and their hybridised wire arrays in the absence of external fields

operating frequencies as also verified in Fig. 13.18b. From this perspective, the observed structure-associated opaqueness arising from the short-cut wires correlated with the transmission enhancement at DNG operating frequencies provide a way out to achieve transmission tunability in the context of engineering metacomposites through manipulation of Co-based wire spacing and its arrangement.

To date, three kinds of hybrid metacomposites are introduced, i.e. dense continuous, dilute continuous, and short-cut metacomposites. It is worth reiterating that, compared with the metacomposite containing single Fe-based wire arrays, hybrid metacomposites demonstrate metamaterial characteristics that are more tunable by external magnetic field. As discussed above, several effects, i.e. FMR in Fe-based wire, Fe–Fe wire, Co–Co wire, and Fe–Co wire interactions, are involved and the predominating mechanism varies at different frequency. A combination of coarse and fine control of metacomposite behaviour is therefore readily available via the selection of different microwires and manipulation of any spacing and arrangement that are involved in this composite system. In view of these merits, the present composite may indicate a significant application of radio frequency identification (RFID), in which structure polymer composites are heavily used. The RFID is a contactless data-capturing technique using RF waves to

automatically identify objects. The ever-increasing applications of RFID for commercial inventory control in warehouses, supermarkets, hospitals as well as military friend-and-foe identification have resulted in considerable research interest on low-cost, long-range sensor design. Conventional RF tags are usually achieved either by the printed spacing-filling curves [112] or by the capacitively tuned dipoles [113]. However, these tags consist of complicated-shaped structure, thus requiring large manufacturing costs. Furthermore, the undesirable parasitic coupling effect of these structures when interacting with EM waves makes the precise analysis of their EM performance rather difficult. Our present study herein proposes a kind of versatile composite containing microwire arrays of a simple structure. By incorporating these wire composites into the objects to be detected, each object will have a unique ID coded in these composites. Moreover, the recent unfortunate "MH370" event calls for application of such multifunctional composites to identify civil airplanes by their distinguished microwave response, considering their DNG features in the radar frequencies. Such application appears to be more practical than cloaking invisibility at this stage, and importantly, for differentiating civil aircrafts from military planes or even identifying every airborne vehicle.

Lastly, the prepreg-based composites possess much better mechanical properties compared to those conventional metamaterials in addition to the metamaterial particularities [114]. Indeed, regardless of the matrix, the wire arrays alone [62] or simply bonding the wire arrays on the paper [74, 115] is able to yield negative permittivity (see Fig. 13.10). But the essential requirement for composites in engineering application is their structural function. In this sense, the proper choice of matrix, fabrication, and the resultant structural performance need to be addressed carefully to obtain a truly applicable multifunctional composite.

References

1. Pendry JB (2000) Negative refraction makes a perfect lens. Phys Rev Lett 85:3966–3969
2. Shalaev VM, Cai W, Chettiar UK, Yuan HK, Sarychev AK, Drachev VP, Kildishev AV (2005) Negative index of refraction in optical metamaterials. Opt Lett 30:3356–3358
3. Alu A, Engheta N (2003) Pairing an epsilon-negative slab with a mu-negative slab: resonance, tunnelling and transparency. IEEE Trans Antennas Propag 51:2558–2571
4. Shelby RA, Smith DR, Schultz S (2001) Experimental verification of a negative index of refraction. Science 292:77–79
5. Smith DR, Padilla WJ, Vier DC, Nemat-Nasser SC, Schultz S (2000) Composite medium with simultaneously negative permeability and permittivity. Phys Rev Lett 84:4184–4187
6. Valentine J, Li J, Zentgraf T, Bartal G, Zhang X (2009) An optical cloak made of dielectrics. Nat Mater 8:568–571
7. Sihvola A (2007) Metamaterials in electromagnetics. Metamaterials 1:2–11
8. http://www.aichi-mi.com/
9. Shamonina E, Solymar L (2007) Metamaterials: how the subject started. Metamaterials 1:12
10. Maier SA (2007) Metamaterials and imaging with surface plasmon polaritons. Springer, New York
11. Dolling G, Wegener M, Linden S, Hormann C (2006) Photorealistic images of objects in effective negative-index materials. Opt Express 14:1842–1849

12. Veselago V (1968) The electrodynamics of substances with simultaneously negative values of ε and μ. Soviet Phys Usp 10:509–514
13. Rotman W (1962) Plasma simulation by artificial dielectrics and parallel-plate media. IRE Trans Anntenas Propag 10:82–95
14. Pendry JB, Holden AJ, Stewart WJ, Youngs I (1996) Extremely low frequency plasmons in metallic mesostructures. Phys Rev Lett 76:4773–4776
15. Lagarkov AN, Matytsin SM, Rozanov KN, Sarychev AK (1998) Dielectric properties of fiber-filled composites. J Appl Phys 84:3806–3814
16. Lagarkov AN, Sarychev AK (1996) Electromagnetic properties of composites containing elongated conducting inclusions. Phys Rev B 53:6318–6336
17. Makhnovskiy DP, Panina LV. (2005) Field and stress tunable microwave composite materials based on ferromagnetic wires. In: Murray VN (ed) Progress in ferromagnetism research. Nova Science Publishers Inc., Hauppauge
18. Fang N, Lee H, Sun C, Zhang X (2005) Sub-diffraction-limited optical imaging with a silver superlens. Science 308:534–537
19. Shalaev VM (2007) Optical negative-index metamaterials. Nat Photon 1:41–48
20. Schurig D, Mock JJ, Justice BJ, Cummer SA, Pendry JB, Starr AF, Smith DR (2006) Metamaterial electromagnetic cloak at microwave frequencies. Science 314:977–980
21. Liu R, Ji C, Mock JJ, Chin JY, Cui TJ, Smith DR (2009) Broadband ground-plane cloak. Science 323:366–369
22. Cai W, Chettiar UK, Kildishev AV, Shalaev VM (2008) Designs for optical cloaking with high-order transformations. Opt Express 16:5444–5452
23. Sato K, Nomura T, Matsuzawa S, Iizuka H (2008) Metamaterial techniques for automotive applications. In: PIERS proceedings, Hangzhou, China, pp 1122–1125, 24–28 Mar 2008
24. Melik R, Unal E, Perkgoz NK, Puttlitz C, Demir HV (2009) Metamaterial-based wireless strain sensors. Appl Phys Lett 95:011106
25. Alici KB, Özbay E (2007) Radiation properties of a split ring resonator and monopole composite. Phys Status Solidi B 244:1192–1196
26. Zou Y, Jiang L, Wen S, Shu W, Qing Y, Tang Z, Luo H, Fan D (2008) Enhancing and tuning absorption properties of microwave absorbing materials using metamaterials. Appl Phys Lett 93:261115
27. Watts CM, Liu X, Padilla WJ (2012) Metamaterial electromagnetic wave absorbers. Adv Mater 24:OP98–OP120
28. Landy NI, Sajuyigbe S, Mock JJ, Smith DR, Padilla WJ (2008) Perfect metamaterial absorber. Phys Rev Lett 100:207402
29. Wakatsuchi H, Christopoulos C (2011) Generalized scattering control using cut-wire-based metamaterials. Appl Phys Lett 98:221105
30. Ourir A, Ouslimani HH (2011) Negative refractive index in symmetric cut-wire pair metamaterial. Appl Phys Lett 98:113505
31. Butt H, Dai Q, Farah P, Butler T, Wilkinson TD, Baumberg JJ, Amaratunga GAJ (2010) Metamaterial high pass filter based on periodic wire arrays of multiwalled carbon nanotubes. Appl Phys Lett 97:163102
32. Wen QY, Zhang HW, Yang QH, Xie YS, Chen K, Liu YL (2010) Terahertz metamaterials with VO_2 cut-wires for thermal tunability. Appl Phys Lett 97:021111
33. Bratkovsky A, Ponizovskaya E, Wang SY, Holmstrom P, Thylen L, Fu Y, Agren H (2008) A metalwire/ quantum-dot composite metamaterial with negative epsilon and compensated optical loss. Appl Phys Lett 93:193106
34. Zhou R, Zhang H, Xin H (2010) Metallic wire array as low-effective index of refraction medium for directive antenna application. IEEE Trans Antennas Propag 58:79–87
35. Gorkunov MV, Osipov MA (2008) Tunability of wire-grid metamaterial immersed into nematic liquid crystal. J Appl Phys 103:036101
36. Cabuz AI, Nicolet A, Zolla F, Felbacq D, Bouchitte G (2011) Homogenization of nonlocal wire metamaterial via a renormalization approach. J Opt Soc Am B Opt Phys 28:1275–1282

37. Dong ZG, Xu MX, Lei SY, Liu H, Li T, Wang FM, Zhu SN (2008) Negative refraction with magnetic resonance in a metallic double-ring metamaterial. Appl Phys Lett 92:064101
38. Falcone F, Martin F, Bonache J, Marques R, Lopetegi T, Sorolla M (2004) Left handed coplanar waveguide band pass filters based on bi-layer split ring resonators. IEEE Microwave Wirel Compon Lett 14:10–12
39. Marqués R, Medina F, Rafii-El-Idrissi R (2002) Role of bianisotropy in negative permeability and left-handed metamaterials. Phys Rev B 65:144440
40. Marques R, Mesa F, Martel J, Medina F (2003) Comparative analysis of edge- and broadside- coupled split ring resonators for metamaterial design - theory and experiments. IEEE Trans Antennas Propag 51:2572–2581
41. Baena JD, Marqués R, Medina F, Martel J (2004) Artificial magnetic metamaterial design by using spiral resonators. Phys Rev B 69:014402
42. Baena J, Bonache J, Martin F, Sillero R, Falcone F, Lopetegi T, Laso M, Garcia-Garcia J, Gil I, Portillo M, Sorolla M (2005) Equivalent-circuit models for split-ring resonators and complementary split-ring resonators coupled to planar transmission lines. IEEE Trans Microwave Theor Techn 53:1451–1461
43. Zhao H, Zhou J, Zhao Q, Li B, Kang L, Bai Y (2007) Magnetotunable left-handed material consisting of yttrium iron garnet slab and metallic wires. Appl Phys Lett 91:131107
44. Zhao H, Zhou J, Kang L, Zhao Q (2009) Tunable two-dimensional left-handed material consisting of ferrite rods and metallic wires. Opt Express 17:13373–13380
45. Pendry JB, Schurig D, Smith DR (2006) Controlling electromagnetic fields. Science 312(5781):1780–1782
46. Vakil A, Engheta N (2011) Transformation optics using graphene. Science 332(6035): 1291–1294
47. Bückmann T, Thiel M, Kadic M, Schittny R, Wegener M (2014) An elasto-mechanical unfeelability cloak made of pentamode metamaterials. Nat Commun 5, doi:10.1038/ncomms5130
48. Pendry JB, Holden AJ, Robbins D, Stewart W (1999) Magnetism from conductors and enhanced nonlinear phenomena. IEEE Trans Microwave Theor Techn 47(11):2075–2084
49. Soukoulis CM, Wegener M (2011) Past achievements and future challenges in the development of three-dimensional photonic metamaterials. Nat Photonics 5(9):523–530
50. Zhu J, Gu H, Luo Z, Haldolaarachige N, Young DP, Wei S et al (2012) Carbon nanostructure-derived polyaniline metacomposites: electrical, dielectric, and giant magnetoresistive properties. Langmuir 28(27):10246–10255
51. Zhu J, Wei S, Zhang L, Mao Y, Ryu J, Mavinakuli P et al (2010) Conductive polypyrrole/tungsten oxide metacomposites with negative permittivity. J Phys Chem C 114(39):16335–16342
52. Guo J, Gu H, Wei H, Zhang Q, Haldolaarachchige N, Li Y et al (2013) Magnetite–polypyrrole metacomposites: dielectric properties and magnetoresistance behavior. J Phys Chem C 117(19):10191–10202
53. Zhu J, Wei S, Zhang L, Mao Y, Ryu J, Karki AB et al (2011) Polyaniline-tungsten oxide metacomposites with tunable electronic properties. J Mater Chem 21(2):342–348
54. Zhu J, Wei S, Ryu J, Guo Z (2011) Strain-sensing elastomer/carbon nanofiber "metacomposites". J Phys Chem C 115(27):13215–13222
55. Vazquez M, Adenot-Engelvin AL (2009) Glass-coated amorphous ferromagnetic microwires at microwave frequencies. J Magn Magn Mater 321:2066–2073
56. Montiel H, Alvarez G, Gutierrez M, Zamorano R, Valenzuela R (2006) The effect of metal-to-glass ratio on the low-field microwave absorption at 9.4 GHz of glass-coated CoFeBSi microwires. IEEE Trans Magn 42(10):3380–3382
57. Phan M, Peng H, Yu S, Wisnom M (2007) Large enhancement of GMI effect in polymer composites containing Co-based ferromagnetic microwires. J Magn Magn Mater 316(2): e253–e256
58. Phan MH, Peng HX (2008) Giant magnetoimpedance materials: fundamentals and applications. Prog Mater Sci 53(2):323–420

59. Qin F, Peng H, Phan M (2010) Wire-length effect on GMI in $Co_{70.3}Fe_{3.7}B_{10}Si_{13}Cr_3$ amorphous glass-coated microwires. Mater Sci Eng B 167(2):129–132
60. Zhukov A, Zhukova V (2009) Magnetic Properties and Applications of Ferromagnetic Microwires with Amorphous and Nanocrystalline Structure. Nova Science Publishers Inc., New York
61. Qin F, Peng H-X (2013) Ferromagnetic microwires enabled multifunctional composite materials. Prog Mater Sci 58(2):183–259
62. Garcia-Miquel H, Carbonell J, Boria V, Sánchez-Dehesa J (2009) Experimental evidence of left handed transmission through arrays of ferromagnetic microwires. Appl Phys Lett 94:054103
63. Chen J, Tang D, Zhang B, Yang Y, Lu M, Lu H, Lu F, Xu W (2007) Left-handed materials made of dilute ferromagnetic wire arrays with gyrotropic tensors. J Appl Phys 102:023106
64. Carbonell J, García-Miquel H, Sánchez-Dehesa J (2010) Double negative metamaterials based on ferromagnetic microwires. Phys Rev B 81:024401
65. Garcia-Miquel H, Carbonell J, Sanchez-Dehesa J (2010) Left handed material based on amorphous ferromagnetic microwires tunable by dc current. Appl Phys Lett 97:094102
66. Labrador A, Gómez-Polo C, Pérez-Landazábal JI, Zablotskii V, nigo Ederra I, Gonzalo R, Badini-Confalonieri G, Vázquez M (2010) Magnetotunable left-handed FeSiB ferromagnetic microwires. Opt Lett 35:2161–2163
67. Sarychev AK, Shalaev VM (2000) Electromagnetic field fluctuations and optical nonlinearities in metal-dielectric composites. Phys Rep 335:275–371
68. Ivanov AV, Shalygin AN, Galkin VY, Vedyayev AV (2009) Rozanov3 KN. Metamaterials with tunable negative refractive index fabricated from amorphous ferromagnetic microwires: magnetostatic interaction between microwires. PIERS. ONLINE 5:649–652
69. Kittel C (1948) On the theory of ferromagnetic resonance absorption. Phys Rev 73:155
70. Adenot-Engelvin AL, Dudek C, Acher O (2005) Microwave permeability of metamaterials based on ferromagnetic composites. J Magn Magn Mater 300:33–37 (The third Moscow international symposium on magnetism 2005)
71. Adenot-Engelvin AL, Dudek C, Toneguzzo P, Acher O (2007) Microwave properties of ferromagnetic composites andmetamaterials. J Eur Ceram Soc 27:1029–1033
72. Qin F, Peng HX, Tang J, Qin LC (2010) Ferromagnetic microwires enabled polymer composites for sensing applications. Compos A Appl Sci Manuf 41:1823–1828
73. Liu L, Kong L, Lin G, Matitsine S, Deng C (2008) Microwave permeability of ferromagnetic microwires composites/metamaterials and potential applications. IEEE Trans Magn 44:3119–3122
74. Panina LV, Ipatov M, Zhukova V, Zhukov A, Gonzalez J (2011) Magnetic field effects in artificial dielectrics with arrays of magnetic wires at microwaves. J Appl Phys 109:053901
75. Makhnovskiy DP, Panina LV, Mapps DJ (2001) Field-dependent surface impedance tensor in amorphous wires with two types of magnetic anisotropy: helical and circumferential. Phys Rev B 63:144424
76. Y DI, Jiang J, Du G, Tian B, Bie S, He H (2007) Magnetic and microwave properties of glass-coated amorphous ferromagnetic microwires. Trans Nonferrous Met Soc China 17:1352–1357
77. Qin FX, Peng HX, Phan MH, Panina LV, Ipatov M, Zhukova V, Zhukov A, Gonzalez J (2011) Smart composites with short ferromagneticmicrowires formicrowave applications. IEEE Trans Magn 47:4481–4484
78. Vazquez M, Chiriac H, Zhukov A, Panina L, Uchiyama T (2011) On the state-of-the-art in magnetic microwires and expected trends for scientific and technological studies. Physica Status Solidi (A) 208:493–501
79. Shinjo T, Shigeto K, Nagahama T, Mibu K, Ono T (2000) Studies on magnetization reversal in submicron wires and domain wall behaviors. J Phys Soc Jpn 69:91–98
80. Otani Y, Kim SG, Fukamichi K, Kitakami O, Shimada Y (1998) Magnetic and transport properties of sub micron ferromagnetic wires. IEEE Trans Magn 34:1096–1098

81. Chiriac H, Corodeanu S, Lostun M, Ababei G, Ovari TA (2010) Magnetic behavior of rapidly quenched submicron amorphous wires. J Appl Phys 107:09A301
82. Ovari TA, Corodeanu S, Chiriac H (2011) Domain wall velocity in submicron amorphous wires. J Appl Phys 109:07D502
83. Chiriac H, Lostun M, Ababei G, Ovari TA (2011) Comparative study of the magnetic properties of positive and nearly zero magnetostrictive submicron amorphous wires. J Appl Phys 109:07B501
84. Saitoh E, Tanaka M, Miyajima H, Yamaoka T (2003) Domain-wall trapping in a ferromagnetic nanowire network. J Appl Phys 93:7444–7446
85. Ono T, Ooka Y, Kasai S, Miyajima H, Nakatani N, Hayashi N, Shigeto K, Mibu K, Shinjo T (2001) Magnetization reversal and electric transport in ferromagnetic nanowires. Mater Sci Eng B-Solid State Mater Adv Technol 84:126–132
86. Chiriac H, Corodeanu S, Lostun M, Stoian G, Ababei G, Ovari TA (2011) Rapidly solidified amorphous nanowires. J Appl Phys 109:063902
87. Kraus L, Infante G, Frait Z, Vazquez M (2011) Ferromagnetic resonance in microwires and nanowires. Phys Rev B 83:174438
88. Vega V, Prida VM, Garcia JA, Vazquez M (2010) Torque magnetometry analysis of magnetic anisotropy distribution in ni nanowire arrays. Physica Status Solidi a-Applications and Materials Science 208:553–558
89. Tartakovskaya EV, Pardavi-Horvath M, Vazquez M (2010) Configurational spin reorientation phase transition in magnetic nanowire arrays. J Magn Magn Mater 322:743–747
90. Gonzalez-Diaz JB, Garcia-Martin JM, Garcia-Martin A, Navas D, Asenjo A, Vazquez M, Hernandez-Velez M, Armelles G (2009) Plasmon-enhanced magneto-optical activity in ferromagnetic membranes. Appl Phys Lett 94:263101
91. Pardavi-Horvath M, Si PE, Vazquez M, Rosa WO, Badini G (2008) Interaction effects in permalloy nanowire systems. J Appl Phys 103:07D517
92. Navas D, Pirota KR, Zelis PM, Velazquez D, Ross CA, Vazquez M (2008) Effects of the magnetoelastic anisotropy in ni nanowire arrays. J Appl Phys 103:07D523
93. Ramos CA, De Biasi E, Zysler RD, Brigneti EV, Vazquez M (2007) "blocking" effects in magnetic resonance? the ferromagnetic nanowires case. J Magn Magn Mater 316:E63–E66
94. Prida VM, Pirota KR, Navas D, Asenjo A, Hernandez-Velez M, Vazquez M (2007) Self-organized magnetic nanowire arrays based on alumina and titania templates. J Nanosci Nanotechnol 7:272–285
95. Gonzalez-Diaz JB, Garcia-Martin A, Armelles G, Navas D, Vazquez M, Nielsch K, Wehrspohn RB, Gosele U (2007) Enhanced magneto-optics and size effects in ferromagnetic nanowire arrays. Adv Mater 19:2643–2647
96. Ivanov A, Galkin VY, Ivanov VA, Petrov DA, Rozanov KN, Shalygin AN, Starostenko SN (2009) Metamaterials fabricated of amorphous ferromagnetic microwires: negative microwave permeability. Solid State Phenom 152–153:333–336
97. Luo Y, Peng HX, Qin FX, Ipatov M, Zhukova V, Zhukov A, Gonzalez J (2013) Fe-based ferromagnetic microwires enabled meta-composites. Appl Phys Lett 103:251902
98. Makhnovskiy D, Zhukov A, Zhukova V, Gonzalez J (2009) Tunable and self-sensing microwave composite materials incorporating ferromagnetic microwires. Adv Sci Technol 54:201–210
99. Luo Y, Peng H, Qin F, Ipatov M, Zhukova V, Zhukov A et al (2014) Metacomposite characteristics and their influential factors of polymer composites containing orthogonal ferromagnetic microwire arrays. J Appl Phys 115(17):173909
100. Vázquez M, Zhukov A (1996) Magnetic properties of glass-coated amorphous and nanocrystalline microwires. J Magn Magn Mater 160:223–228
101. Qin F, Peng H-X, Tang J, Qin L-C (2010) Ferromagnetic microwires enabled polymer composites for sensing applications. Compos A Appl Sci Manuf 41(12):1823–1828

102. Sampaio L, Sinnecker E, Cernicchiaro G, Knobel M, Vázquez M, Velázquez J (2000) Magnetic microwires as macrospins in a long-range dipole-dipole interaction. Phys Rev B 61 (13):8976
103. Velázquez J, García C, Vázquez M, Hernando A (1996) Dynamic magnetostatic interaction between amorphous ferromagnetic wires. Phys Rev B 54(14):9903
104. Velázquez J, Vazquez M, Hernando A (1999) Interacting amorphous ferromagnetic wires: a complex system. J Appl Phys 85(5):2768–2774
105. Kraus L, Frait Z, Ababei G, Chiriac H (2013) Ferromagnetic resonance of transversally magnetized amorphous microwires and nanowires. J Appl Phys 113(18):183907–183908
106. García-Miquel H, Carbonell J, Sánchez-Dehesa J (2010) Left handed material based on amorphous ferromagnetic microwires tunable by dc current. Appl Phys Lett 97(9):094102–094103
107. García-Miquel H, Carbonell J, Boria V, Sánchez-Dehesa J (2009) Experimental evidence of left handed transmission through arrays of ferromagnetic microwires. Appl Phys Lett 94 (5):054103
108. Luo Y, Qin F, Scarpa F, Carbonel J, Ipatov M, Zhukova V et al (2015) Hybridized magnetic microwire metacomposites towards microwave cloaking and barcoding applications. ArXiv Preprint arXiv:150607745
109. Makhnovskiy D, Panina L, Garcia C, Zhukov A, Gonzalez J (2006) Experimental demonstration of tunable scattering spectra at microwave frequencies in composite media containing CoFeCrSiB glass-coated amorphous ferromagnetic wires and comparison with theory. Phys Rev B 74(6):064205
110. Qin F, Peng H, Fuller J, Brosseau C (2012) Magnetic field-dependent effective microwave properties of microwire-epoxy composites. Appl Phys Lett 101(15):152905
111. Luo Y, Peng H, Qin F, Adohi B, Brosseau C (2014) Magnetic field and mechanical stress tunable microwave properties of composites containing Fe-based microwires. Appl Phys Lett 104(12):121912
112. McVay J, Hoorfar A, Engheta N (2006) Space-filling curve RFID tags. In: Radio and wireless symposium. IEEE, pp 199–202
113. Jalaly I, Robertson I (2005) Capacitively-tuned split microstrip resonators for RFID barcodes. In: Microwave conference, European, vol 2. IEEE, 4pp
114. Peng H, Qin F, Phan MH, Tang J, Panina L, Ipatov M, Zhukov A, Zhukova V, Gonzalez J (2009) Cobased magnetic microwire and field-tunable multifunctional macro-composites. J Non-Cryst Solids 355:1380–1386
115. Panina L, Ipatov M, Zhukova V, Zhukov A, Gonzalez J (2010) Microwave metamaterials with ferromagnetic microwires. Appl Phys A Mater Sci Process 103:653–657